JOURNAL OF MATERIALS SCIENCE 24 (1989) 4467–4474

Fabrication and sinterability in Y_2O_3–CeO_2–ZrO_2

J. G. DUH, M. Y. LEE
Department of Materials Science and Engineering, National Tsing Hua University, Hsinchu 30043, Taiwan

CeO_2-stabilized tetragonal zirconia polycrystal (Ce–TZP) containing 1 to 6 mol % $YO_{1.5}$ have been fabricated as fine powders by a coprecipitation technique. The microstructure of the as-sintered surface and fracture surface were examined by electron microscopy. CeO_2 dopants reduced the phase transformation temperature from amorphous to tetragonal and stabilized the tetragonal phase at low temperature. The addition of Y_2O_3 to Ce–TZP inhibited the grain growth. The sintered density reached 99% theoretical for short sintering times at 1440 and 1540° C, but decreased slightly to 97 to 98% theoretical for longer sintering times. The decrease in density is attributed to the morphological development of agglomerates, which induce large pores during sintering. The average grain size decreased significantly as the yttrium content increased from 1 to 3 mol %. Specimens aged in water at low temperatures exhibited no phase transformation. This implies fairly good thermal stability in the Y_2O_3-doped Ce–TZP system.

1. Introduction

The application of zirconia-based ceramics is extended to many aspects of advanced materials because of its good mechanical, thermal, chemical and electrical properties. To use zirconia to its full potential, the properties of the oxide have been modified by the addition of stabilizing dopants, such as MgO, CaO, Y_2O_3 and CeO_2 [1–7]. High-performance zirconia ceramics depend on the microstructure. Yttria-doped tetragonal zirconia polycrystals (Y-TZP) are attractive because of their excellent mechanical properties, wear properties and thermal expansion coefficients close to those of iron-based alloys [8–10]. The high strength and fracture toughness of TZP is considered to be caused by the stress-induced transformation from tetragonal to monoclinic phase [11]. However, degradation in mechanical properties have been reported during low-temperature ageing in air or in humid atmospheres [12–17]. The CeO_2–ZrO_2 system has better thermal stability and higher toughness than Y–TZP [18–20]. The strength of Ce–TZP is, however, relatively low and requires further development to present a challenge to Y-TZP.

A recent study on the synthesis and sintering behaviour in the CeO_2–ZrO_2 system has been reported [7]. In the present investigation, yttria-doped Ce–TZP was employed to probe the effect of yttria dopant on the sinterability. The average grain size after sintering was evaluated by scanning electron microscopy and the phase was examined by X-ray diffraction. The ceramic powder was fabricated through a chemical process to have a controlled grain size during sintering. In addition, a low-temperature ageing test was conducted to evaluate the thermal stability in the Y_2O_3–CeO_2–ZrO_2 system.

2. Experimental procedure

The powder preparation in this study was based on the coprecipitation method. The detailed procedure is shown in the flow chart of Fig. 1. $ZrOCl_2 \cdot 8H_2O$, $Ce(NO_3)_3 \cdot 6H_2O$, and $Y(NO_3)_3 \cdot 5H_2O$ (Merck & Co. Inc., Darmstadt, West Germany) were used to prepare stock solutions. The concentrated ammonia solution was added dropwise to the well-stirred solution mixture until a coprecipitate was formed. The coprecipitate was vacuum filtered after each preparation, washed with deionized water to remove chloride ions, and then dehydrated with alcohol three times. After dehydration, the gel was ground in a hot mortar and pestle under an infrared lamp until a dry powder was obtained. Table I lists the compositions of the samples employed in this study.

The as-fabricated powder was calcined at 500° C for 1 h. X-ray phase analysis and crystalline size determination were preformed with a X-ray diffractometer equipped with copper radiation at 30 kV and 20 mA (Rigaku, Geigerflex D/MAX-B, Japan). X-ray scans of 2 θ between 27° and 33° were conducted to estimate the monoclinic to tetragonal ratio, while those between 72° and 75° were used to discriminate between the tetragonal and cubic phases. The volume fraction of monoclinic phase was estimated according to the Equation [21]

$$V_m = \frac{1.311 X_m}{1 + 0.311 X_m} \quad (1)$$

TABLE I Compositions of the samples employed in this study

Sample designation	Composition (mol %)
0Y	$10CeO_2 - ZrO_2$
1Y	$1 YO_{1.5} - 10CeO_2 - ZrO_2$
2Y	$2 YO_{1.5} - 10CeO_2 - ZrO_2$
3Y	$3 YO_{1.5} - 10CeO_2 - ZrO_2$
4Y	$4 YO_{1.5} - 10CeO_2 - ZrO_2$
5Y	$5 YO_{1.5} - 10CeO_2 - ZrO_2$
6Y	$6 YO_{1.5} - 10CeO_2 - ZrO_2$

0022–2461/89 $03.00 + .12

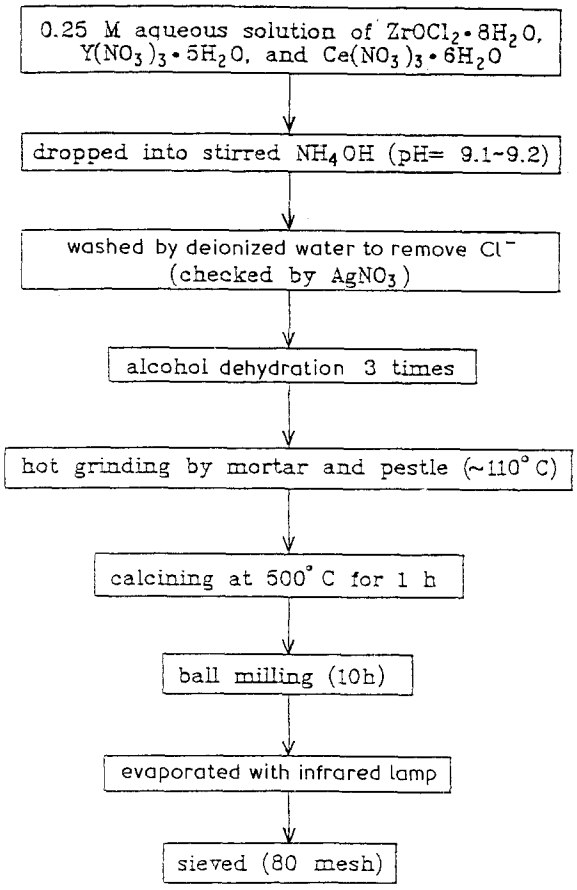

Figure 1 Prepartion of yttria-doped Ce-TZP powders.

where V_m is the volume fraction of monoclinic phase and X_m is the integrated intensity ratio defined as

$$X_m = \frac{I_{m(1\,1\,1)} + I_{m(1\,1\,\bar{1})}}{I_{m(1\,1\,1)} + I_{m(1\,1\,\bar{1})} + I_{t(1\,1\,1)}}$$

where subscripts m and t represent the monoclinic and tetragonal phase, respectively.

The mean crystalline size of the calcined powder was calculated from the breadth at half peak height through the Scherrer relationship [22]. In this work, the $(1\,1\,1)_t$ line of zirconia was used for size measurement. Instrumental broadening was measured through scanning diffraction peaks of a sintered Ce-TZP pellet of which the grain size is greater than 1 μm.

The powders were pressed into pellets with 1 cm diameter under a pressure of 150 MPa. The green density was about 40% theoretical. The sintering experiment was carried out in air in an alumina muffle furnace (Linberg) at 1440 and 1540° C, respectively, from 1 to 8 h. The bulk density was measured by Archimedes' technique with distilled water as the immersion median. The lattice parameters were measured by X-ray Debye–Scherrer camera with silicon as a standard material.

The microstructure of the as-sintered and fracture surfaces was examined with a scanning electron microscope (Hitachi S-570, Japan). The average grain size of the sample was estimated according to the method proposed by Mendelsohn [23].

Low-temperature annealing experiments in water were performed in sealed stainless tubes. The sintered ceramics were put into the tubes and 30 ml deionized water was added. The tube was sealed and placed in a furnace at temperatures of 150 and 250° C, respectively. The sealed tubes were removed from the furnace after 1 wk and 1 mon, respectively, followed by water quenching to room temperature. The annealed specimens were examined by X-ray diffraction to see if any phase transformation had occurred during the ageing process.

3. Results and discussion

3.1. X-ray analysis

The as-fabricated powder shows no crystalline phase when examined by X-ray diffraction. Fig. 2 shows the X-ray diffraction pattern for sample 3Y. No crystalline phase is observed for the as-synthesized gel. However, at temperatures as low as 330° C, a small amount of tetragonal crystalline is nucleated. A broad peak with 2θ values ranging from 27° to 32° indicates the tetragonal phase. The intensity of this peak increases as the calcination temperature is raised from 380 to 500° C. As compared to the results in pure ZrO_2 and yttria-doped ZrO_2 [24], this implies that the addition of CeO_2 to the ZrO_2 system decreases the phase transformation temperature and tends to stabilize the tetragonal phase at low temperatures.

The crystalline size of the powder calcined at

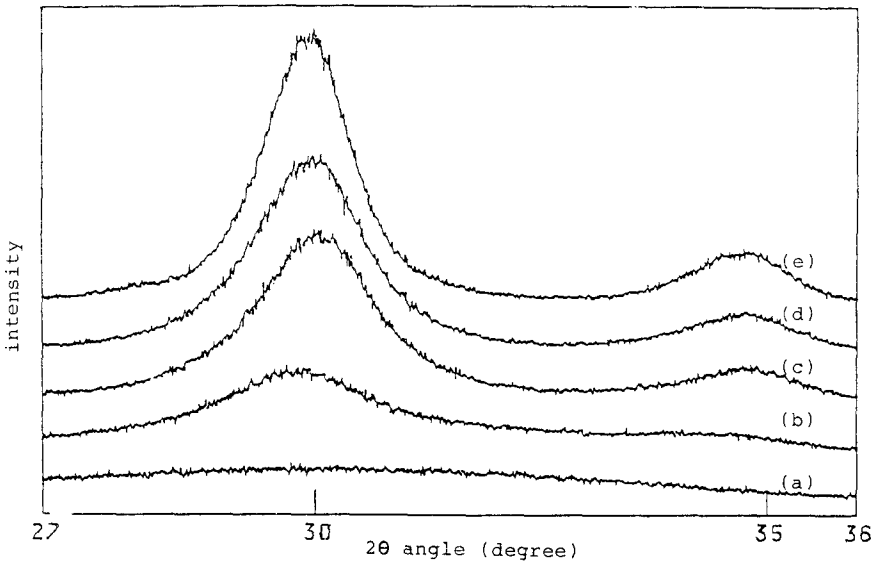

Figure 2 X-ray diffraction patterns of 3 mol % $YO_{1.5}$–10 mol % CeO_2–ZrO_2 powders uncalcined and calcined at various temperatures for 1 h: (a) gel, (b) 330° C, (c) 380° C, (d) 400° C and (e) 500° C.

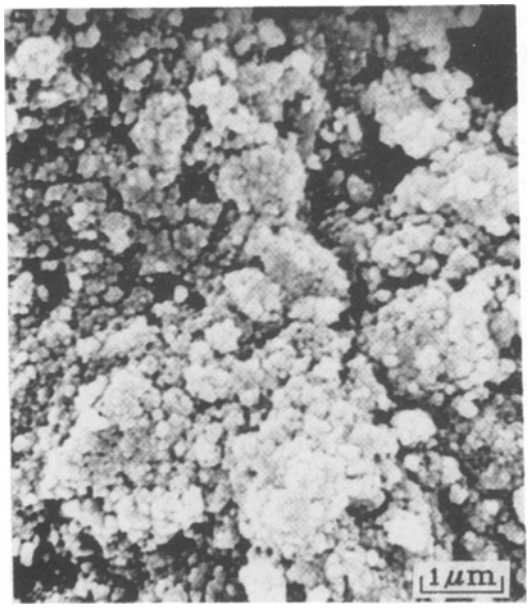

Figure 3 SEM image of the fracture surface of the green pellet uniaxially pressed under a pressure of 150 MPa.

different temperatures was calculated using Scherrer's relationship [22]

$$D = K\lambda/B \cos \theta \quad (4)$$

where D is the average crystalline dimension, λ is the X-ray wavelength, B is the corrected line width at half maximum of the peak, θ is the Bragg angle and K is the crystalline shape factor. The shape factor, K, is chosen arbitrarily as unity in this study. The calculated crystalline sizes are given in Table II. The crystalline size increases with increasing calcination temperature.

3.2. Sintering behaviour

The as-fabricated powders were uniaxially cold-pressed into pellets of 1 cm diameter under a pressure of 150 MPa. The relative green density was about 40%. Fig. 3 shows a scanning electron micrograph of the fracture surface of the green pellet.

Figs 4 and 5 present the relative density after sintering for the Y_2O_3-doped Ce–TZP (tetragonal zirconia polycrystal) at 1440 and 1540° C, respectively. The sintered densities are all greater than 98% when sintered at 1440° C for several hours. Except for the specimen 1Y, the sintered density fails to increase up to 8 h sintering. At 1540° C sintering, the density decreases when the sintering time increases to 8 h. For samples 1Y, 4Y and 6Y, the density is only around 97%. Similar behaviour was observed by Sato and Shimada [19] and Smith and Baumard [25]. Sato and Shimada proposed that the decrease in density for long sintering times was due to the formation of

TABLE II Crystalline size estimated from XRD at various calcination temperatures

	Calcination temperature (° C)					
	380	400	430	460	500	1300
Crystalline size (nm)	6.7	6.8	7.5	8.0	8.4	42.1
Phase	T*	T	T	T	T	T

*T: tetragonal phase.

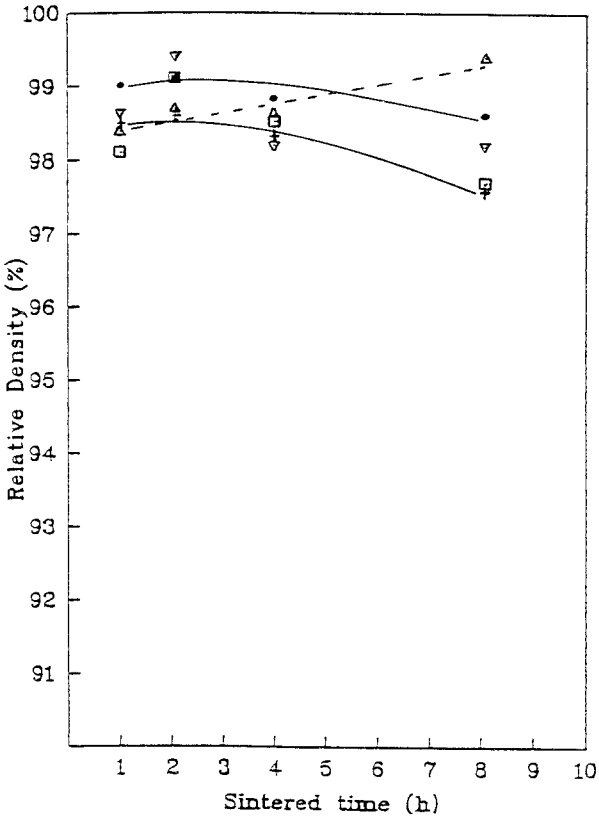

Figure 4 Relative density of the yttria-doped Ce–TZP specimens as a function of sintering time at 1440° C. (●) 1 $YO_{1.5}$, (+) 2 $YO_{1.5}$, (△) 3 $YO_{1.5}$, (▽) 4 $YO_{1.5}$, (□) 6 $YO_{1.5}$.

microcracking accompanied by the tetragonal to monoclinic phase transformation during cooling. In this study, if microcracking is dominant in the densification process, the fraction of monoclinic phase would be 20 to 30% corresponding to the relative

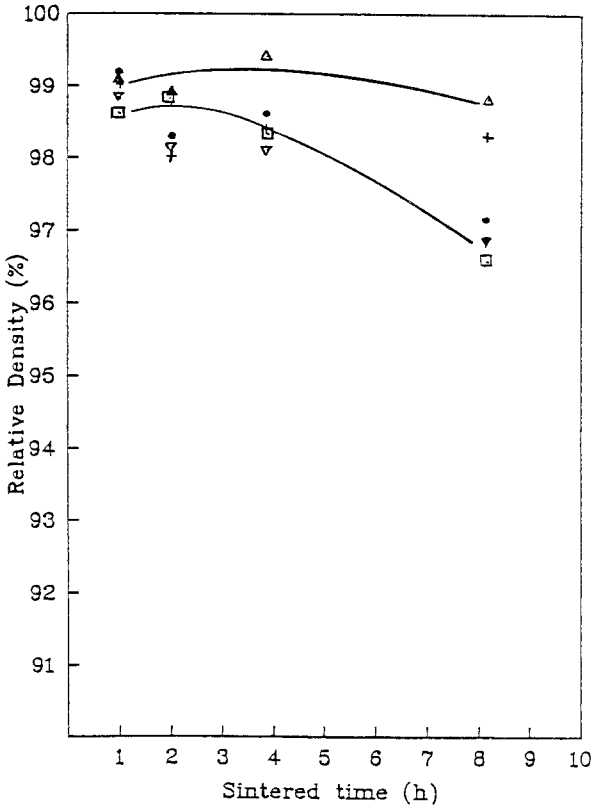

Figure 5 Relative density of the yttria-doped Ce–TZP specimens as a function of sintering time at 1540° C. For key see Fig. 4.

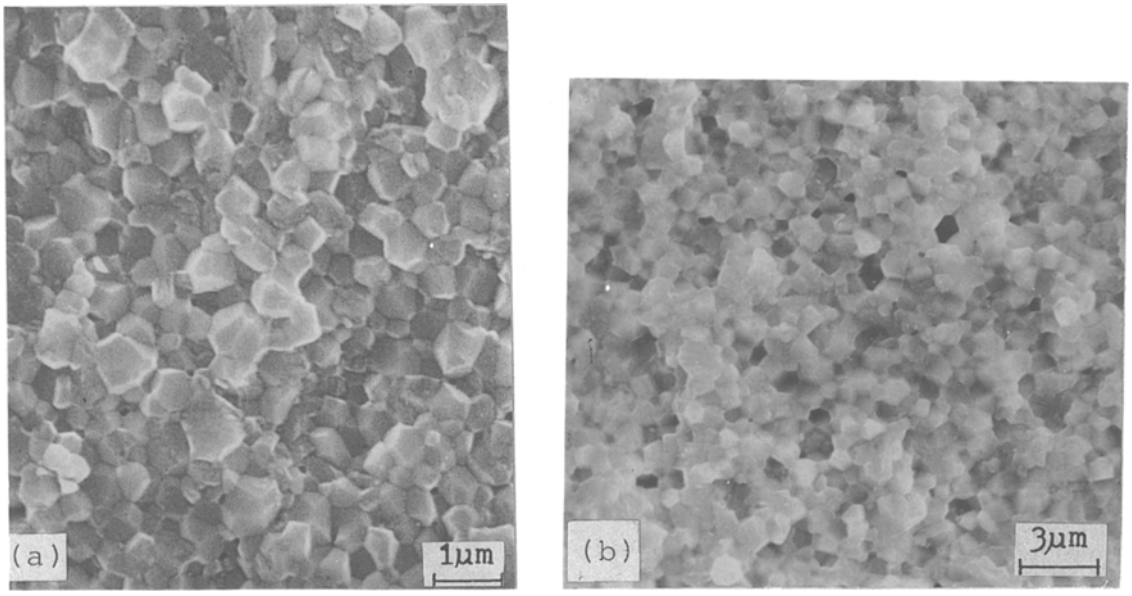

Figure 6 SEM image of the fracture surface of specimen 3Y sintered at 1440° C for (a) 2 h, (b) 8 h.

density decreasing from 99% to 97%, because the volume expansion of tetragonal → monoclinic transformation is 3 to 5%. However, no monoclinic phase is detected for the samples employed in Figs 4 and 5. This strongly suggests that microcracking is not the major factor in the decrease of the density after sintering for a long time. The concepts of pore distribution presented by Lange [26] and agglomeration of the powders are introduced to illustrate the sintering behaviour in this work.

The sintering matrix can be divided into two categories with respect to the microstructure of sintering. One is the sintering of the *intra*-agglomerate; the other is the sintering of the *inter*-agglomerate. The diffusion distance of ions is shorter in the intra-agglomerate than that in the case of inter-agglomerate, as the crystalline contacts are closer in the intra-agglomerate. In the early stage of sintering, intra-agglomerates shrink faster than inter-agglomerates. Highly densified agglomerates are formed as shown in Fig. 6a, and the density increases to the maximum around 99%. As the sintering time increases, pores on the grain boundary gradually agglomerate at a grain corner as illustrated in Fig. 6b. In the later stage of sintering, the densified agglomerate pulls away from neighbouring agglomerates leaving large voids. The agglomerates protrude above the specimen's surface, enlarging the volume of the specimen, and thus decreasing the relative density.

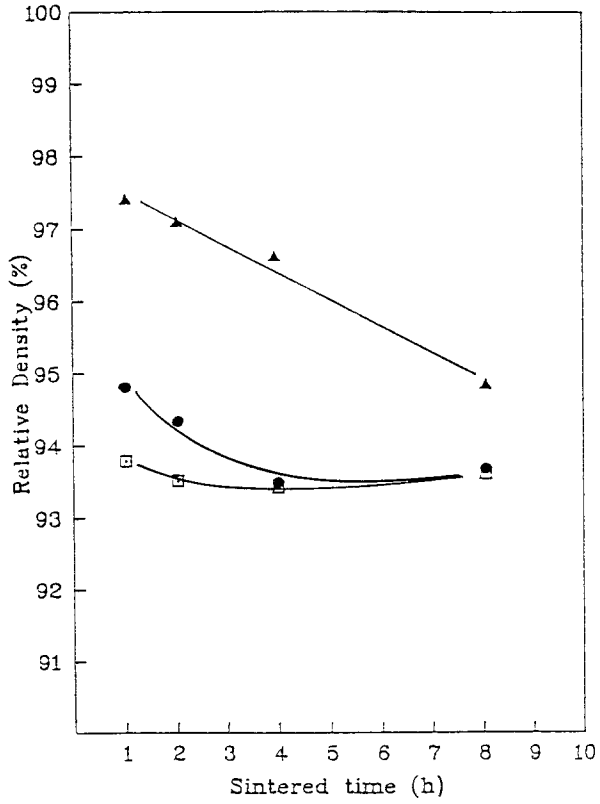

Figure 7 Relative density of the 10 mol % CeO_2–ZrO_2 specimen as the function of the sintering time at (▲) 1350, (●) 1440 and (⊡) 1540° C.

The sintering behaviour of Y_2O_3-free Ce–TZP was also investigated. Fig. 7 shows the relative density of a 10 mol % CeO_2–ZrO_2 sample sintered at 1350, 1440 and 1540° C, for times ranging from 1 to 8 h. Similar to the results for Y_2O_3–CeO_2–ZrO_2 as shown in Fig. 5, the density does not increase with sintering time for one specific sintering temperature. The relatively poor density is attributed to the spontaneous transformation from tetragonal to monoclinic phase on cooling. Cracks induced by phase transformation are observed across the sintered specimen, as indicated in Fig. 8. Typical scanning electron micrographs of the as-sintered surface are shown in Fig. 9. The fracture mode is intergranular. As the sintering temperature is raised or the sintering time is increased, the decrease in sintered density is due to the increase in the volume fraction of the monoclinic phase, as discussed below.

3.3. Phase and grain size

Table III lists the volume fraction of monoclinic phase in the Y_2O_3-free Ce–TZP sample calculated using Equation 1. The large amount of monoclinic phase is due to large grains in the specimen which transform from tetragonal to monoclinic phase spontaneously. The average grain size was examined by the intercept method. Fig. 10 shows the relationsip between the

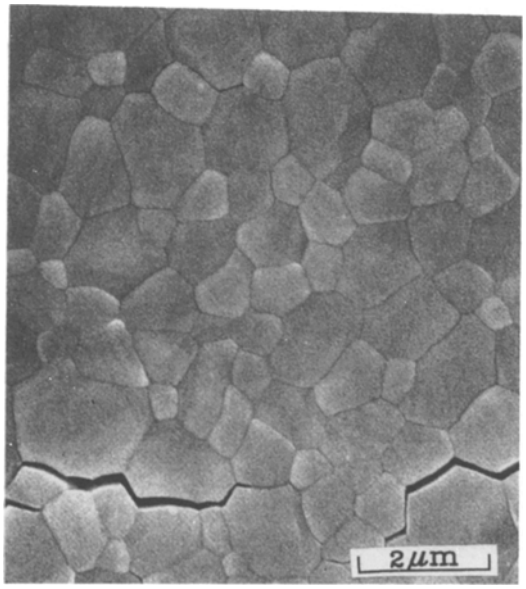

Figure 8 SEM image of the as-sintered surface for the 10 mol % CeO_2–ZrO_2 specimen sintered at 1540° C for 1 h. A crack is visible.

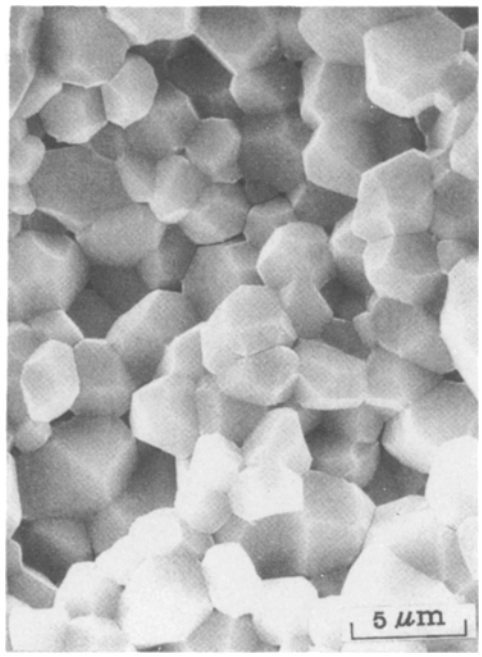

Figure 9 SEM image of the fracture surface for the 10 mol % CeO_2–ZrO_2 specimen sintered at 1540° C for 2 h.

volume fraction of monoclinic phase and the average grain size. The amount of monoclinic phase increases with increasing average grain size. The grain-size effect associated with thermodynamics of constrained transformation was proposed by Lange [27]. Grain-size effects on phase transformation have been studied on partially stabilized zirconia (PSZ) and ZrO_2–Al_2O_3 composite materials by several investigators [10, 28–30]. These studies revealed that the transformation temperature decreased with decreasing grain size, which indicated that the retained tetragonal phase compound of small grains was more stable than that composed of large grains. The critical grain size for the retention of the tetragonal phase of the Ce–TZP was reported by Tsukuma and Shimada [18], which indicated that the critical grain size of 10 mol % Ce–TZP was about 1 μm. In this study, the specimen of 10 mol % Ce–TZP sintered at 1350° C for 1 h has an average grain size about 0.3 μm with 60% monoclinic phase. The difference may be due to the lack of a pyrochlore-type compound, $(La, Nd)_2Zr_2O_7$, or the different sintering schedule compared to Tsukuma and Shimada's work.

The phase determined by X-ray diffraction analysis of the as-sintered surface shows that almost all Y_2O_3-doped Ce–TZP is tetragonal phase. Only specimen 6Y exhibits a small amount of cubic phase. The (4 0 0) peak of the cubic phase was detected by the X-ray diffraction method as shown in Fig. 11. The average grain sizes of Y_2O_3-doped Ce–TZP sintered at 1440° C and 1540° C for 1, 2, 4 and 8 h are represented in Figs 12 and 13, respectively. These data indicate that the average grain size is strongly affected by the composition, sintering temperature and time. In comparison with the average grain size of Y_2O_3-free Ce–TZP [6, 7, 18], the presence of yttria tends to inhibit grain growth. After 1440° C sintering, the average grain size decreases significantly as the concentration of yttrium increases from 1 to 3 mol %. On the other hand, the average grain size slightly increases as the yttrium content increases from 4 to 6 mol %. Similar trend prevails at 1540° C sintering. Lange [31] suggested that the cubic phase controlled the grain growth of the tetragonal phase. The SEM image of the fracture surface of specimen 6Y shows the transgranular fracture surface of large cubic grains as indicated in Fig. 14. The size of the cubic grains is a factor of 5 to 10 larger than tetragonal grains. Ruhle *et al.* [9] argued that cubic grains were not single phase, but themselves contained small tetragonal precipitates of 10 nm diameter. The tetragonal precipitates presented in these large cubic grains might have precipitated during cooling following the sintering. The phase stability of the tetragonal phase depends on composition, temperature and grain size. The underlying theory has been discussed by many investigators [27, 32, 33]. Y_2O_3 addition decreases the Gibbs free energy of tetragonal phase, inhibits the grain growth and leads to a critical grain size larger than 1 μm. Thus highly metastable tetragonal phase at room temperature is obtained, as observed in the present study.

TABLE III Volume fraction of monoclinic phase in 10 mol % CeO_2–ZrO_2

Time (h)	Temperature (° C)		
	1350	1440	1540
1	57.5%	87.9%	93.6%
2	70.7%	92.3%	95.7%
4	73.8%	90.8%	93.8%
8	83.8%	93.4%	93.5%

3.4. Ageing test

All the specimens with different yttrium contents were annealed in distilled water at low temperatures 150 and 250° C for 1 wk and 1 mon, respectively. After heat treatment, specimens were examined by X-ray diffraction, which revealed that no phase transformation occurred. This result indicates that Y_2O_3-doped

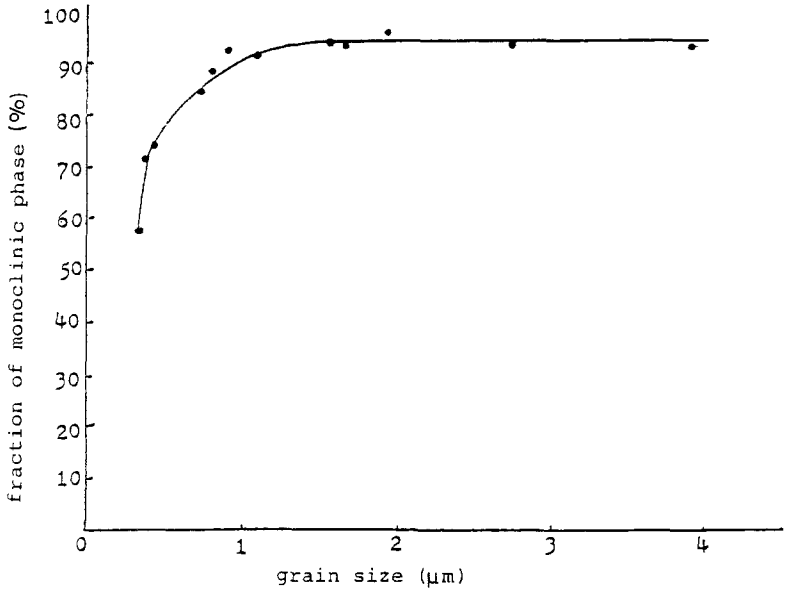

Figure 10 The fraction of the monoclinic phase for the 10 mol % CeO_2–ZrO_2 specimen as a function of grain size.

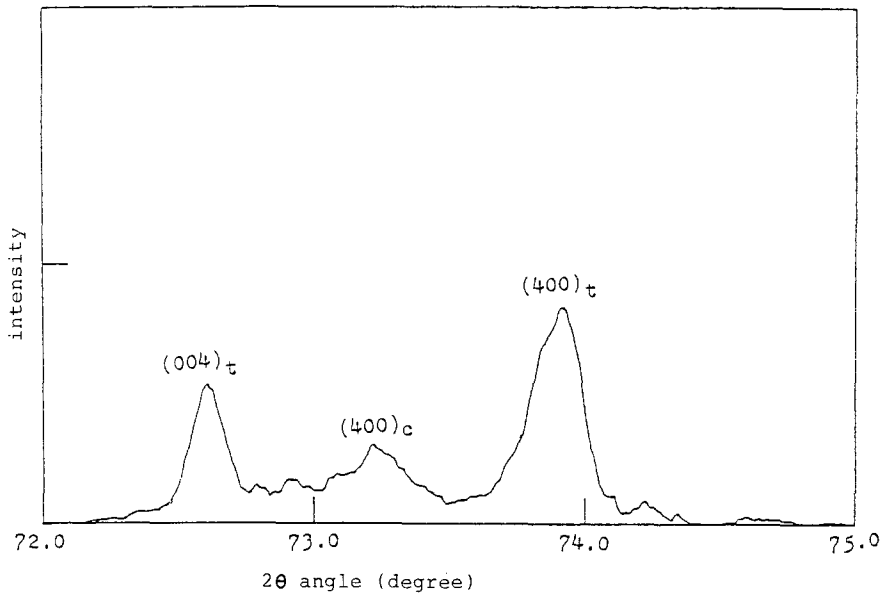

Figure 11 X-ray diffraction pattern for specimen 6Y. A small $(400)_c$ peak is detected.

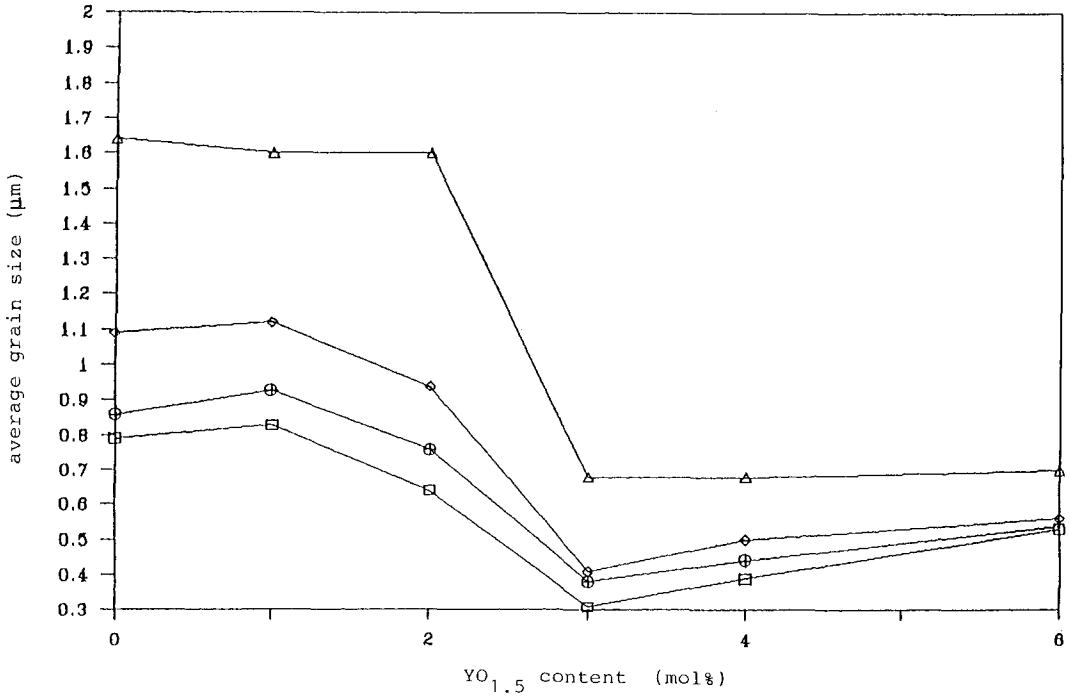

Figure 12 Average grain size as a function of $YO_{1.5}$ content for specimens sintered at 1440° C, for (□) 1 h, (○) 2 h, (◇) 4 h, (△) 8 h.

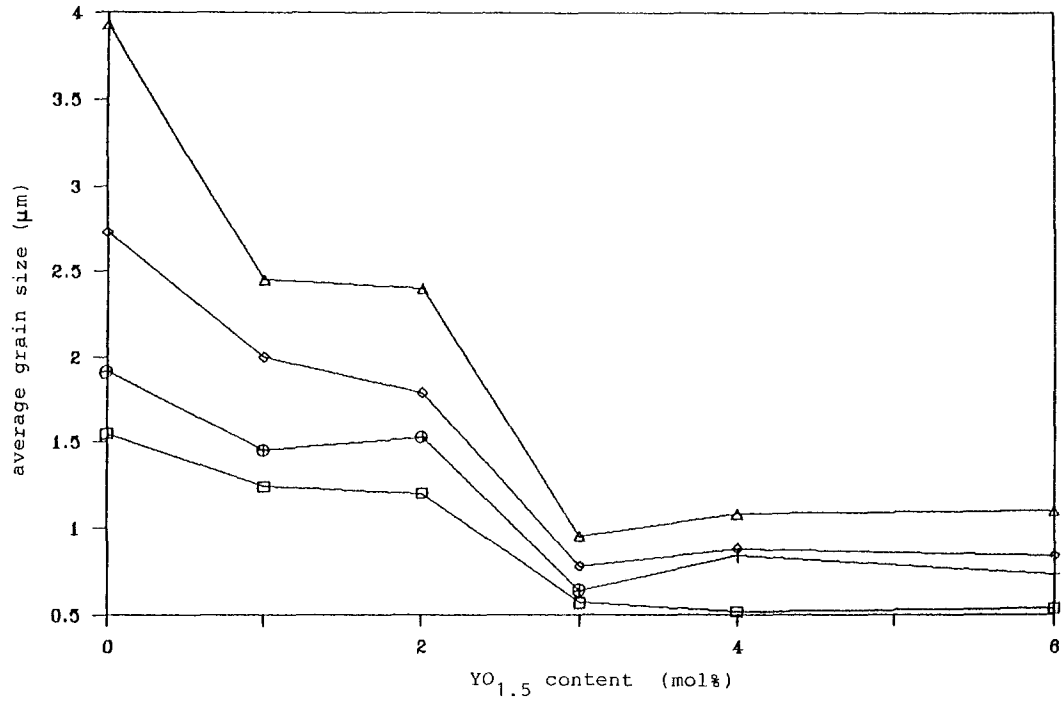

Figure 13 Average grain size as a function of $YO_{1.5}$ content for specimens sintered at 1540° C. For key see Fig. 12.

Ce–TZP possesses better thermal stability than Y–TZP as reported by other workers [13–17].

4. Conclusions

1. Dense Ce–TZP containing 1 to 6 mol % $YO_{1.5}$ were fabricated as fine powders by a coprecipitation technique.

2. CeO_2 dopants in ZrO_2 reduce the phase transformation temperature from amorphous to tetragonal and stabilize the tetragonal phase at low temperature. The as-calcined powder is in the fully tetragonal phase.

3. The addition of Y_2O_3 to the Ce–TZP system inhibits grain growth and further decreases the phase transformation temperature from tetragonal to monoclinic phase.

4. The sintered density reaches 99% theoretical for short sintering time at 1440 and 1540° C, while it decreases slightly to 97 to 98% theoretical up to 8 h sintering. The decrease in density may be attributed to agglomerates pulling away from neighbouring agglomerates, leaving large pore during the last stage of sintering.

5. The grain size in Y_2O_3-doped Ce–TZP is affected by the composition, sintering temperature and sintering time. The average grain size decreases significantly as the concentration of yttrium increases from 1 to 3 mol %. The critical grain size for phase transformation is larger than 2 μm.

6. After low-temperature ageing in water, specimens examined by X-ray diffraction exhibit no phase transformation. This suggests fairly good thermal stability of the Y_2O_3-doped Ce–TZP specimen.

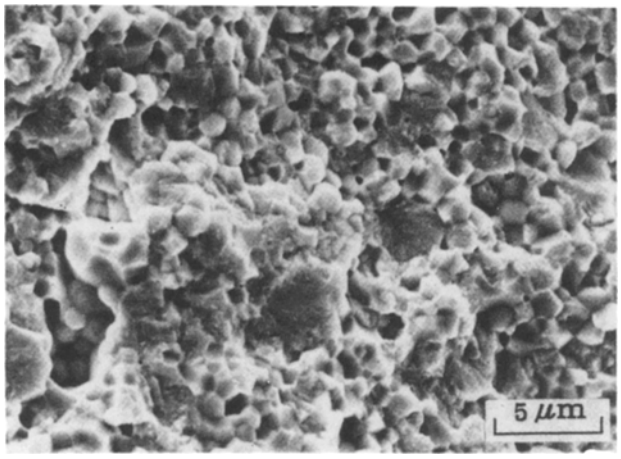

Figure 14 Sem image of fracture surface for specimen 6Y sintered at 1540° C for 4 h.

Acknowledgement

The authors are grateful for the financial support from National Science Council, Taiwan under contracts no. NSC76-0405-E007-12 and NSC77-0405-E007-26R.

References

1. C. T. GRAIN, *J. Amer. Ceram. Soc.* **50** (1967) 288.
2. M. G. SCOTT, *J. Mater. Sci.* **10** (1975) 1527.
3. R. A. MILLER, J. L. SMIALEK and R. G. GARLICK, in "Advances in Ceramics", Vol. 3, "Science and Technology of Zirconia", edited by A. H. Heuer and L. W. Hobbs (The American Ceramic Societly, Columbus, Ohio, 1981) p. 241.
4. J. M. MARDER, T. E. MITCHELL and A. H. HEUER, *Acta Metall.* **31** (1983) 387.
5. D. L. PORTER and A. H. HEUER, *J. Amer. Ceram. Soc.* **62** (1979) 298.
6. T. W. COYLE, W. S. COBLENZ and B. A. BENDER, *Amer. Ceram. Soc. Bull.* **62** (1983) 966.
7. J. G. DUH, H. T. DAI and W. Y. HSU, *J. Mater. Sci.* **23** (1988) 2786.
8. T. K. GUPTA, J. H. BECHTOLD, R. C. KUZNICKIE, L. H. CADOFF and B. R. ROSSING, *ibid.* **12** (1977) 2421.
9. M. RUHLE, N. CLAUSSEN and A. H. HEUER, in "Advances in Ceramics", Vol. 12, "Science and Technology of Zirconia II", edited by N. Claussen, M. Ruhle and A. H. Heuer (American Ceramic Society, Columbus, Ohio, 1984) p. 352.
10. F. F. LANGE, *J. Mater. Sci.* **17** (1982) 240.

11. *Idem, J. Amer. Ceram. Soc.* **61** (1978) 85.
12. K. KOBAYASHI, H. KUWAJIMA and T. MASAKI, *Solid State Ionics* **3–4** (1981) 489.
13. T. SATO and M. SHIMADA, *J. Amer. Ceram. Soc.* **68** (1985) 356.
14. T. MASAKI, *Int. J. High Tech. Ceram.* **2** (1986) 85.
15. F. F. LANGE, G. L. DUNLOP and B. I. DAVID, *J. Amer. Ceram. Soc.* **69** (1986) 237.
16. M. WATANABE, S. IIO and I. FUNKURA, in "Advances in Ceramics", Vol. 12, edited by N. Claussen, M. Ruhle and A. A. Heuer (American Ceramic Society, Columbus, Ohio 1984) p. 391.
17. K. TSUKUMA and M. SHIMADA, *J. Mater. Sci. Lett.* **4** (1985) 857.
18. *Idem, J. Mater. Sci.* **20** (1985) 1178.
19. T. SATO and M. SHIMADA, *Amer. Ceram. Soc. Bull.* **64** (1985) 1382.
20. J. G. DUH, H. T. DAI and B. S. CHIOU, *J. Amer. Ceram. Soc.* **71**(10) (1988) 813.
21. H. TORAYO, M. YOSHIMURA and S. SOMIYA, *ibid.* **67** (1984) C-119.
22. B. D. CULLITY, "Elements of X-ray Diffraction" 2nd Edn (Addison-Wesley, Reading, Massachusetts, 1978) p. 102.
23. M. I. MENDELSOHN, *J. Amer. Ceram. Soc.* **52** (1969) 443.
24. R. C. GARVIE, *J. Phys. Chem.* **69** (1965) 1238.
25. A. SMITH and J. F. BAUMARD, *Amer. Ceram. Soc. Bull.* **66** (1978) 1144.
26. F. F. LANGE, *J. Amer. Ceram. Soc.* **67** (1984) 83.
27. *Idem, J. Mater. Sci.* **17** (1982) 225.
28. *Idem, ibid.* **17** (1982) 237.
29. F. F. LANGE and D. J. GREEN, in "Advances in Ceramics", Vol. 3, Science and Technology of Zirconia I", edited by A. H. Heuer and L. W. Hobbs (American Ceramic Society, Columbus, Ohio, 1981) p. 217.
30. R. H. J. HANNINK, K. A. JOHNSTON, R. T. PASCOE and R. C. GARVIE, *ibid.* p. 116.
31. F. F. LANGE, *J. Amer. Ceram. Soc.* **69** (1986) 240.
32. A. G. EVANS and R. M. CANNON, *Acta Metall.* **34** (1986) 761.
33. R. J. SEYLER, S. LEE and S. J. BURNS, in "Advances in Ceramics", Vol. 12, "Science and Technology of Zirconia II", edited by N. Claussen, M. Ruhle and A. H. Heuer (American Ceramic Society, Columbus, Ohio, 1984) p. 213.

Received 9 November 1988
and accepted 31 January 1989